Organics on Mars : Laboratory studies of organic material under simulated martian conditions

Kate, Inge Loes ten

Chapter 3

Amino acid photostability on the martian surface

In the framework of international planetary exploration programmes several space missions are planned that will search for organics and bio-signatures on Mars. Previous attempts have not detected any organic compounds in the martian regolith. It is therefore critical to investigate the processes that may affect organic molecules on and below the planet's surface. Laboratory simulations can provide useful data about the reaction pathways of organic material at Mars' surface. We have studied the stability of amino acid thin films against ultraviolet (UV) irradiation, and we use those data to predict the survival time of these compounds on and in the martian regolith. We show that thin films of glycine and D-alanine are expected to have a half-life of 22 ± 5 hours and of 3 ± 1 hours, respectively, when irradiated with Mars-like UV flux levels. Modelling shows that the half-lives of the amino acids are extended to the order of 10^7 years when embedded in regolith. These data suggest that subsurface sampling must be a key component of future missions to Mars dedicated to organic detection.

Inge Loes ten Kate, James R. C. Garry, Zan Peeters, Richard Quinn, Bernard H. Foing, Pascale Ehrenfreund
Meteoritics and Planetary Science 2005; 40(5):1185-1193

1. INTRODUCTION

In the apparent absence of biogenic processes on the martian surface, exogenous delivery of organic material must be taken into account. Organic compounds are present in certain classes of meteorites as well as in comets (Ehrenfreund *et al.*, 2002). Intact extraterrestrial delivery of such organic material could have been a significant factor in determining the organic make-up of early Earth and Mars (Pierazzo and Chyba, 1999; Ehrenfreund *et al.*, 2002). Flynn and McKay (1990) have estimated that the mass of meteoritic material reaching the surface of Mars is between 1.63×10^{-6} and 7.36×10^{-8} kg m^{-2} yr^{-1}. The major carbon component in carbonaceous meteorite samples is in the form of insoluble organic macromolecules. In the soluble fraction of such samples more than 70 extraterrestrial amino acids have been identified in addition to many other organic compounds, including N-heterocycles, carboxylic acids, sulphonic and phosphonic acids, and aliphatic and aromatic hydrocarbons (Botta and Bada, 2002; Sephton, 2002, and references therein). The total abundance of all amino acids in the Murchison meteorite was determined to be 17-60 ppm by Botta and Bada (2002). Ehrenfreund *et al.* (2001a) determined that the average of the amino acid abundance in the CI carbonaceous chondrites Orgueil and Ivuna is 5 ppm. If burial processes are ignored, then unaltered carbon compounds should accumulate with an annual flux of ~15 ng m^{-2} yr^{-1}. This flux level should yield detectable concentrations after a geologically brief period. However, the Viking gas chromatograph-mass spectrometer (GCMS), which had an average detection limit on the order of part per billion (ppb), failed to find organic compounds that had not been identified as background contaminates (Biemann *et al.*, 1977). It is thus thought that some process may be at work on Mars that destroys the infalling organic matter, and gaseous oxidizing agents have been postulated as encouraging the destruction of meteoritically delivered organic matter. However, impacting organic matter may be displaced into deeper regolith layers and thus be protected from radiation and oxidation. It is therefore possible that organic meteoritic material is destroyed on the exposed surface, but may survive when protected at depth. The detection of organic material arising from either biotic or abiotic sources, as well as the characterization of oxidants at the martian surface (Zent and McKay, 1994), are among the main goals of future Mars missions.

Laboratory simulations are a crucial step in understanding the chemical pathways on the martian surface (ten Kate *et al.*, 2003). Organic compounds that are abundant in meteorites such as carbonaceous chondrites are a logical target for those experiments since they may have accumulated to form significant deposits on the martian surface via exogenous delivery (Bland and Smith, 2000). We therefore have examined the photostability of the simpler amino acids, given their well-characterized properties and their ubiquitous presence in meteoritic samples. This paper discusses photostability measurements on two amino acids, glycine and D-alanine, exposed to Mars-like UV radiation. D-alanine is used in this study to prevent biological contamination of the samples; the issue of chirality will not be addressed in this paper. The experimental section describes our simulation chamber, as

well as the UV sources used for the irradiation studies. Also described are the experimental procedure and the characterisation of thin films. In the results section we report on the IR spectroscopy of irradiated amino acids samples. Furthermore we tabulate the half-lives and UV destruction cross sections calculated from different experiments and predict the values for martian insolation intensity.

2. Equipment and experimental procedure

The amino acids glycine (99.7% purity, Merck) and D-alanine (98% purity, Sigma) were ground using a pestle and mortar. The powders were loaded into a vacuum sublimation system that holds a set of four silicon discs at a distance of 15 cm above a resistively heated copper oven. Each disc (24 mm diameter, 0.8 mm thick) was polished on both circular faces and permanently fixed to a steel backing ring, with an inner diameter of 1 cm, large enough for the beam of an infrared spectrometer to pass through. Four copper straps, one per disc, have embedded magnets to hold the silicon discs above the sublimation oven and permit the discs to be handled without touching their coated faces.

The sublimation took place under vacuum, at a typical pressure $<3 \times 10^{-4}$ mbar and at an oven temperature between 150 and 175 °C. During the deposition process the layer thickness was monitored using standard laser interferometry. A schematic drawing of the arrangement is shown in Fig. 1. Absolute thickness of the layers was obtained from atomic force microscopy (AFM, Zeiss AxioPlan 2) scans, which also showed that the films formed as solid pore-free layers of nanocrystals. The sublimation rate of the solid amino acid, and hence the layer thickness, was controlled by moderating the

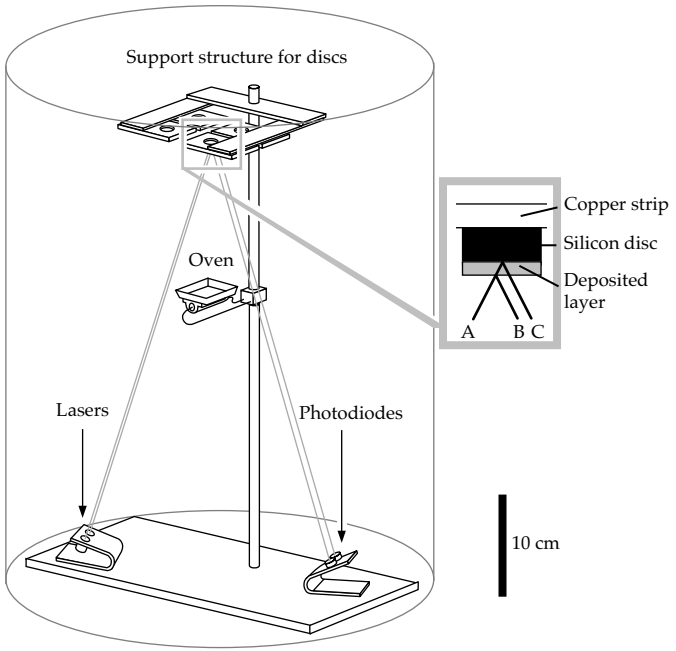

Fig. 1. A schematic drawing of the sublimation chamber, showing the laser geometry. The film thickness can be estimated from the interference arising from the optical path difference taken by rays AC and AB.

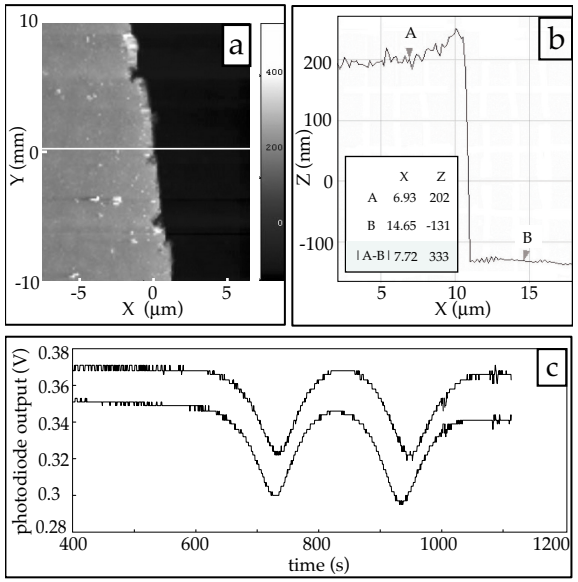

Fig. 2. (a) AFM image of a solid D-alanine layer; the light grey part on the left side is the D-alanine layer, the dark part on the right is the silicon disc on which the layer is deposited. (b) A height profile measurement of the layer along the horizontal line plotted in 2a. (c) The corresponding interferogram from the layer deposition, with two traces showing deposition on the edge (upper trace) and on the centre of the disc (lower trace).

oven heater current. A limited amount of H_2O molecules may be trapped in the amino acid films during deposition, this will be discussed later.

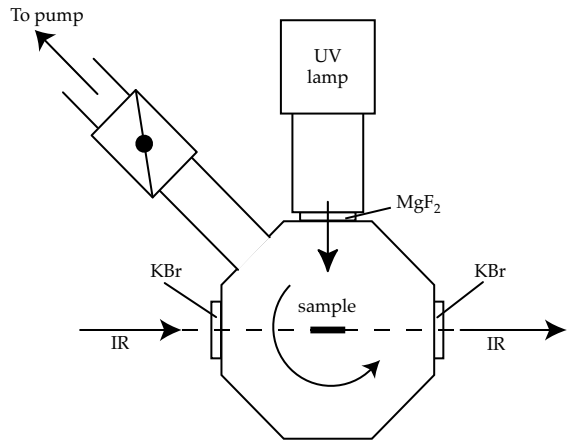

Fig. 3. A schematic drawing of the simulation chamber.

The charts in Fig. 2 show the data for a ~330 nm thick D-alanine layer along with representative data that show that two areas on the disc experience near-identical deposition rates. The thickness of the layer is calculated from the number of interference fringes in the interferogram, not from the ab - solute voltage of the photodiode output.

Although four discs can be coated simultaneously in the sublimation chamber, only one can be accommodated in the simulation chamber, which is shown schematically in Fig. 3.

The body of this small stainless steel chamber is equipped with four ports and a rotary feedthrough. A mounting stage is fixed to the internal end of the feedthrough, and the copper support tabs of the silicon discs can be clamped to this stage.

One of the ports is equipped with a polished magnesium fluoride (MgF_2) window, to admit the light from the UV lamps. On the opposite face of the chamber a clear window is mounted with which the disc's alignment can be verified. The remaining two ports on the chamber hold potassium bromide (KBr) windows that allow the beam from a Fourier Transform infrared (FTIR) spectrometer to pass through the chamber. By turning the rotary feedthrough on the chamber, the disc can be exposed first to UV radiation, and then to the beam of the FTIR spectrometer. Before, during, and after the irradiation phase, absorption spectra were taken using an Excalibur FTS-4000 infrared spectrometer (BioRad) in the range 4000 to 500 cm^{-1} at 4 cm^{-1} resolution.

2.1 UV sources

Two UV sources have been used for the experiments. A microwave-excited hydrogen flow lamp (Opthos) with an average flux of 4.6×10^{14} photons s^{-1} cm^{-2} is used to provide UV light between 120 and 180 nm. The flux of this lamp was measured by solid-state actinometry as described by Cottin *et al.* (2003) and has an estimated uncertainty of 25 %. The second UV source is a deuterium discharge lamp (Heraeus-Noblelight, DX 202, range 190-400 nm). This lamp's output was measured before and after each experiment with a UV sensor

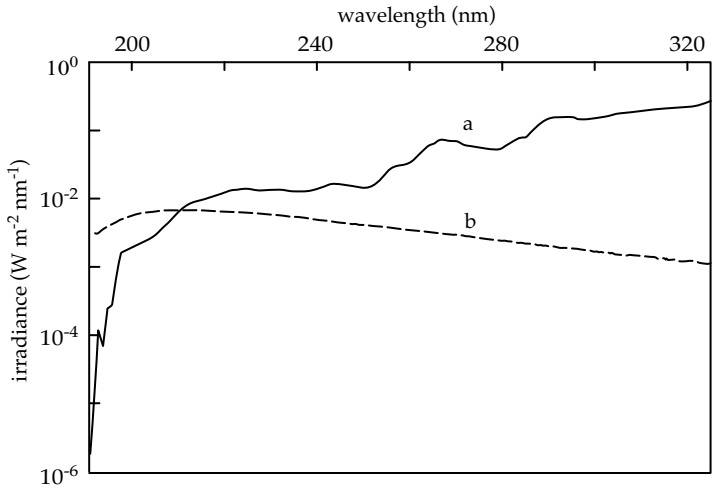

Fig. 4. A comparative chart of the irradiance of the surface noon lighting at the equator of Mars (from Patel *et al.*, 2002) (a), and the light delivered at the working distance of 145 mm from the discharge region of the deuterium lamp (b).

(Solartech model 8.0) that displayed the integrated intensity over the range from ~245 nm to ~265 nm (half-peak sensitivity, full-width). From the known response curve, the irradiance spectrum provided by Heraeus in arbitrary units could be transformed to give spectral irradiance in absolute units. Similarly, the UV sensor could be used to calculate the absolute irradiance spectrum as a function of distance from the lamp. In Fig. 4 the irradiance of the deuterium lamp is shown for a distance of 145 mm from the lamp's discharge point. At

this distance, and over the range of 190 nm to 325 nm, the lamp generates $4.9 \pm 1 \times 10^{13}$ photons s^{-1} cm^{-2} and delivers an intensity of 40 ± 5 μW cm^{-2}. If this intensity is compared to the predicted noontime equatorial insolation at Mars' surface in a low atmospheric dust scenario (Patel *et al.*, 2002), then the deuterium lamp provides ~4 % of the UV experienced on Mars in the range of 190 nm to 325 nm. The spectral profile of the lamp is deficient in the longer wavelengths compared to the solar spectrum. The spectrum of this lamp is shown in Fig. 4 along with a curve showing the lighting spectrum as expected to exist on Mars.

2.2 Experiments

Two sets of experiments have been performed using two amino acids. In the first set of experiments we used the hydrogen flow lamp as a light source. From those experiments, photo-destruction rates of solid glycine and D-alanine can be calculated. The discs were irradiated with the hydrogen flow lamp for 2.5 hours and IR absorption spectra of the layers were recorded during this period. In the second set of experiments the deuterium discharge lamp was used; this lamp has a lower total power output than the hydrogen lamp and longer exposures (> 40 h) were needed to cause measurable destruction. During all of the experiments the irradiation chamber was pumped continuously and had an average internal pressure of 4×10^{-6} mbar.

An early concern was that the layer material may be lost by sublimation during irradiation of the disc. Thus, a separate experiment was conducted to measure the *in situ* temperature of the silicon disc during the irradiation process with both the hydrogen lamp and the deuterium lamp. A Pt100 temperature sensor was glued to the illuminated face of the disc and showed that while lit and under high vacuum the temperature of the disc increased by no more than 2 °C over the course of a three-hour hydrogen lamp exposure and by no more than 10 °C during a 65-hour deuterium lamp exposure. These temperature rises are far below the sublimation temperatures of 150 to 175 °C found for the glycine and D-alanine powders in our sublimation chamber at similar pressures. Also a separate 28-hour experiment has been performed to measure the effect of high vacuum (4×10^{-6} mbar) alone on D-alanine and no change in the layer's absorption spectrum could be seen.

UV spectra of the glycine and D-alanine thin films have been recorded with a Varian Cary 3 Bio UV-Visible spectrophotometer (see Fig. 7). The thin films were deposited on MgF_2 windows, because of its transparency in the short wavelength range, from 120 to 7000 nm. Silicon is not transparent for wavelengths shorter than 1000 nm.

3. Results

We have measured IR spectra of glycine and D-alanine sublimated as thin films onto silicon substrate discs. To confirm the obtained absorption data and perform band assignments the glycine spectra were compared with spectra for glycine in KBr pellets as measured by Ihs *et al.* (1990), Uvdal *et al.*

Table 1. Band assignments and wavenumbers (in cm^{-1}) of some spectral features of the IR spectra of glycine and D-alanine. The labels refer to the peaks in Fig. 5.

Label	Glycine		D-alanine	
	Wavenumber	Band assignment[a]	Wavenumber	Band assignment[a]
a	1599	ν_{as} (COO) [b,c,d]	1623	δ (NH_3) [e,g], ν_{as} (COO) [g]
b	1519	δ_s (NH_3) [b,c,d]	1587	ν_{as} (COO) [e,f,g], δ (NH_3) [g]
c	1446	δ_{sc} (CH_2) [b,c,d]	1456	δ_{as} (CH_3) [e,g]
d	1414	ν_s (COO) [b,c,d]	1414	ν_s (COO) [e]
e	1336	ρ_w (CH_2) [b,c,d]	1360	δ_a (CH_3) [g]
f	916	ρ_r (CH_2) [d]	1307	δ (CH) [f,g]
g	896	δ_{sc} (CC) [d]	1239	β (NH_3) [g]
h	703	ρ_r (COO) [d]	1115	ρ (NH_3) [g]
i			1015	ν_s (CCNC) [g]
j			919	ν_a (CCNC), ρ (CH_3) [g]
k			850	2ν (CCNC), ρ (CH_3) [g]

[a] Approximate description of the band assignment: $\nu_{as/s}$, asymmetric/symmetric stretching; $\beta_{as/s}$, asymmetric/symmetric bending; $\delta_{as/s}$, asymmetric/symmetric deformation; δ_{sc}, scissoring mode; $\rho_{w/r}$, wagging/rocking mode.
[b] Ihs *et al.* (1990); [c] Uvdal *et al.* (1990); [d] Rosado *et al.* (1998); [e] Cao and Fischer (1999); [f] Cao and Fischer (2000); [f] Rozenberg *et al.* (2003).

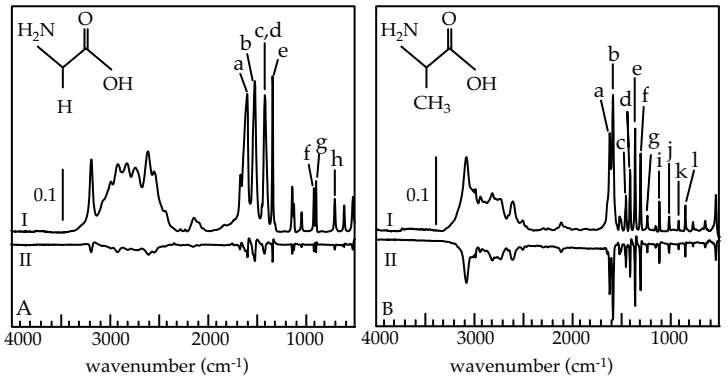

Fig. 5. The IR spectra of (A) solid glycine and (B) solid D-alanine in the range 4000-500 cm^{-1}, measured with a resolution of 4 cm^{-1}. Two spectra are shown, (I) is recorded before irradiation with a deuterium discharge lamp, and (II) is obtained by subtracting the spectrum of the unirradiated compound from the spectrum recorded after 48.3 h (for glycine) and 50.2 h (for D-alanine) of irradiation. The vertical scale bars show the infrared absorbance in arbitrary units. The identification of the peaks can be found in Table 1.

(1990) and Rosado *et al.* (1998). The D-alanine spectra were compared with spectra of L-alanine in KBr pellets determined by Cao and Fischer (1999, 2000) and Rozenberg *et al.* (2003). IR spectra of D- and L-alanine are similar, because chirality does not effect IR spectroscopy (Yamaguchi *et al.*, 2005).
In Fig. 5 glycine and D-alanine infrared absorption spectra before irradiation are shown together with a trace showing the changes in their spectra after ~48 hours of irradiation with

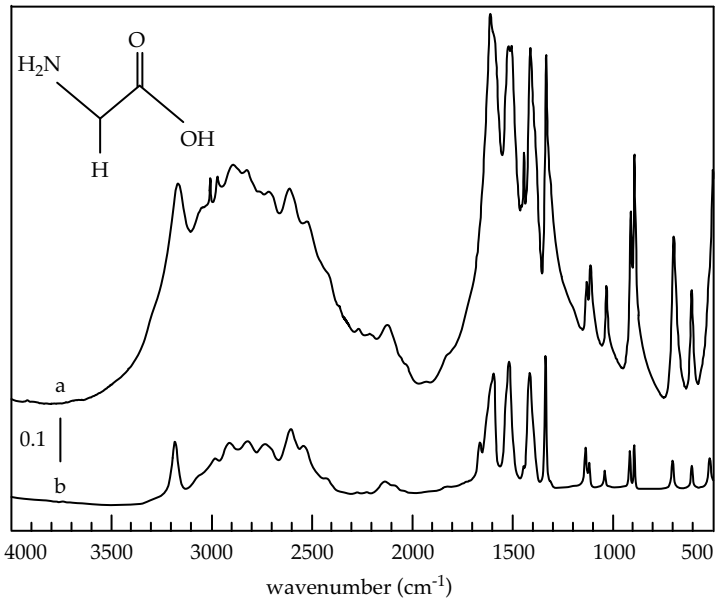

Fig. 6. The IR spectra of (a) glycine in a KBr pellet and (b) solid glycine on a silicon disc, in the range 4000-500 cm^{-1}, measured with a resolution of 4 cm^{-1}. The vertical scale bar shows the infrared absorbance in arbitrary units.

the deuterium lamp. Table 1 describes the band assignments of the main peaks that can be observed in the glycine and D-alanine spectra. A comparison of the IR spectra of glycine in a KBr pellet and a solid layer of glycine on a silicon disc is given in Fig. 6, to show their similarity.

An assumption used in the data processing is that the amino acid films are optically thin. We used the UV sensor to measure the amount of UV light from the deuterium lamp that was reflected from a silicon disc with and without a D-alanine coating. Silicon has an average reflectivity of ~70 % (Edwards, 1985) for light in the wavelength range of 120 nm to 325 nm. This modest reflectivity was confirmed by measurements with the UV sensor, which additionally showed

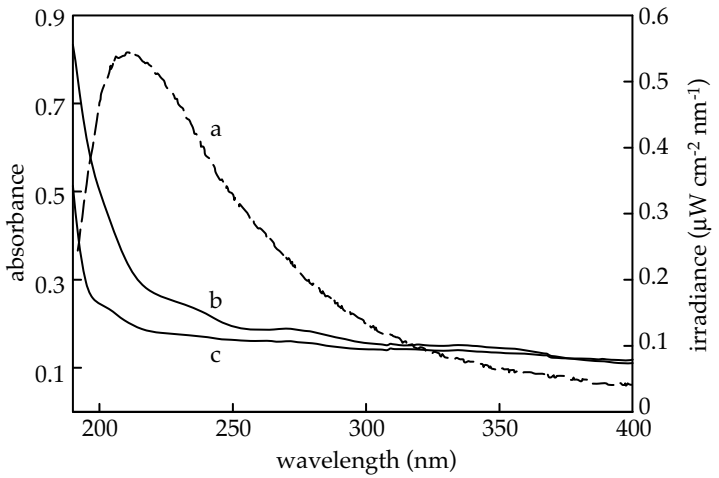

Fig. 7. (a) The spectrum of the deuterium lamp between 190 and 400 nm, recorded at the same distance from the lamp as the amino acid film, scaled to the right ordinate. The UV-visible absorption spectra of a ~300 nm layer of (b) solid glycine and (c) solid D-alanine on a silicon disc, in the range 190 to 400 nm, scaled to the left ordinate.

that the addition of a 250 ± 10 nm thick layer lowered the reflectivity by ~10 % in the spectral window to which the sensor was responsive (245 through 265 nm, half-peak sensitivity, full-width). Absorption spectra of glycine and D-alanine (Fig. 7) at UV and visible wavelengths suggest that comparable amounts of light would be reflected back through the amino acids films at wavelengths other than those measured by the UV sensor. The thickness of the layers and the reflectivity of the silicon substrate also meant that an additional illumination flux of ~65 % had to be considered from photons that pass through the layer and are then reflected by the disc back into the amino acid layer.
With the optically-thin assumption verified, first order reaction kinetics (Cottin *et al.*, 2003) were applied to calculate the half-life and the UV destruction cross section of the solid

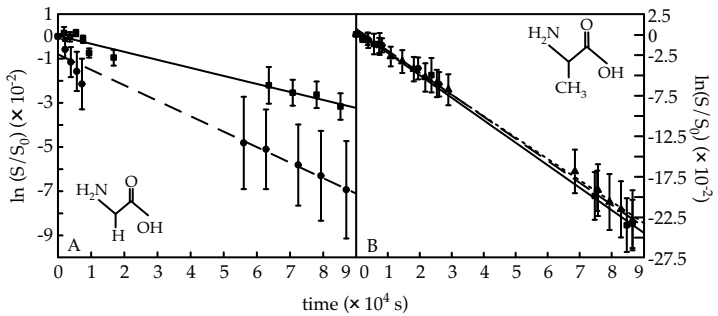

Fig. 8. The natural logarithm of the normalised integrated absorbance ($\ln(S/S_0)$) plotted against time, for the deuterium irradiation of (A) glycine (Table 4), and (B) D-alanine (Table 5).

glycine and D-alanine. The destruction rate is the slope of a linear fit through the natural logarithm of the normalised integrated absorbance plotted against time (Fig. 8). For these calculations the absorbance data of the peaks described in Table 1 are used. From the destruction rate the UV destruction cross section, σ, and the half-life are calculated (Cottin *et al.*, 2003).

In Table 2 and 3 the UV destruction cross sections and the half-lives are compiled for the hydrogen lamp irradiation of glycine and D-alanine. UV photodestruction of matrix isolated glycine has been measured previously by Ehrenfreund *et al.* (2001b) and Peeters *et al.* (2003). These data, however, cannot be directly compared to UV photodestruction of solid thin films. Tables 4 and 5 contain these values for the deuterium lamp irradiation of glycine and D-alanine. In our experiments all of the amino acid layers had thicknesses in the range of 160 to 400 nm. From our experiments it appears, as expected from an optically thin layer, that the layer thickness within this range does not influence the degradation cross section, and the half-life.

The uncertainty in the destruction cross section is dominated by two sources. First, the uncertainty of the hydrogen flow discharge lamp is estimated to be 25 % by Cottin *et al.* (2003) and no appropriate independent sensors were available to confirm this number. Secondly, the calibration certificate of the UV sensor used to calibrate the deuterium UV lamp states an ± 10 % accuracy, and in use the deuterium lamp is stable to better than 1 % of its output when measured over multiple

Table 2: glycine irradiated by the hydrogen flow lamp

experiment	σ (cm^2/molecule)	half-life (s)
1	$2.1 \pm 0.5 \times 10^{-19}$	$4.3 \pm 0.2 \times 10^{3}$
2	$1.6 \pm 0.4 \times 10^{-19}$	$5.9 \pm 0.3 \times 10^{3}$
3	$1.6 \pm 0.4 \times 10^{-19}$	$5.8 \pm 0.2 \times 10^{3}$
4	$3.8 \pm 1.0 \times 10^{-19}$	$2.5 \pm 0.2 \times 10^{3}$
5	$2.9 \pm 0.7 \times 10^{-19}$	$3.2 \pm 0.7 \times 10^{3}$
average	$2.4 \pm 1.5 \times 10^{-19}$	$4.4 \pm 0.6 \times 10^{3}$

Table 3: D-alanine irradiated by the hydrogen flow lamp

experiment	σ (cm^2/molecule)	half-life (s)
1	$2.9 \pm 0.7 \times 10^{-19}$	$3.2 \pm 0.2 \times 10^{3}$
2	$1.3 \pm 0.4 \times 10^{-19}$	$7.1 \pm 0.9 \times 10^{3}$
3	$2.1 \pm 0.7 \times 10^{-19}$	$4.3 \pm 0.9 \times 10^{3}$
4	$3.6 \pm 0.9 \times 10^{-19}$	$2.6 \pm 0.1 \times 10^{3}$
average	$2.5 \pm 1.4 \times 10^{-19}$	$4.3 \pm 1.3 \times 10^{3}$

Table 4: glycine irradiated by the deuterium discharge lamp

experiment	σ (cm^2/molecule)	half-life (s)
1	$5.7 \pm 1.1 \times 10^{-25}$	$1.5 \pm 0.2 \times 10^{6}$
2	$4.1 \pm 0.9 \times 10^{-25}$	$2.2 \pm 0.4 \times 10^{6}$
average	$4.9 \pm 1.4 \times 10^{-25}$	$1.8 \pm 0.4 \times 10^{6}$

Table 5: D-alanine irradiated by the deuterium discharge lamp

experiment	σ (cm^2/molecule)	half-life (s)
1	$3.1 \pm 1.0 \times 10^{-24}$	$2.8 \pm 0.8 \times 10^{5}$
2	$3.1 \pm 1.0 \times 10^{-24}$	$2.8 \pm 0.8 \times 10^{5}$
3	$2.9 \pm 0.6 \times 10^{-24}$	$3.0 \pm 0.3 \times 10^{5}$
average	$3.0 \pm 1.5 \times 10^{-24}$	$2.9 \pm 1.2 \times 10^{5}$

Table 6: half-lives of glycine and D-alanine in the laboratory set-up and extrapolated to Mars' equatorial surface irradiation at local noon.

compound	half-life in our lab set-up (s)	half-life on Mars (s)
glycine	$1.8 \pm 0.4 \times 10^{6}$	$8.0 \pm 1.8 \times 10^{4}$
D-alanine	$2.9 \pm 1.2 \times 10^{5}$	$1.2 \pm 0.5 \times 10^{4}$

days. The overall uncertainty in the measured output of the deuterium lamp is estimated to be ± 15 %. Besides the uncertainties in the lamp flux, smaller uncertainties are taken into account reflecting the error in the linear fit that represents the destruction rate of the amino acid layers.
The half-lives calculated from the laboratory data for the deuterium lamp irradiation of both glycine and D-alanine were extrapolated to Mars' surface UV flux levels. Using data from a model for the martian atmosphere with a low dust-load (Patel *et al.*, 2002) an intensity of 930 μW cm^{-2} was calculated for the wavelength range of 190 nm to 325 nm. This UV flux was used to calculate the half-lives of glycine and D-alanine shown in Table 6.

4. Discussion

Amino acids, the building blocks of proteins, are easily formed and can be well-characterized by different analytical methods. More than 70 different amino acids have been observed in meteorites (Botta and Bada, 2002). Many of these amino acids show isotopic excess confirming their extraterrestrial origin (Sephton, 2002, and references therein). We do not have any evidence for biogenic processes on Mars. If life as we know it developed in certain environments on Mars, amino acids may be present.
We have studied the survival of amino acids exposed to Mars-like UV conditions in the laboratory. In these experiments we found half-lives of $1.8 \pm 0.4 \times 10^{6}$ s and $2.9 \pm 1.2 \times 10^{5}$ s for glycine thin films and D-alanine thin films, respectively, which correspond to half-lives of 22 ± 5 hours and 3 ± 1 hours for glycine and D-alanine, respectively, at Mars UV flux levels. The difference in measured destruction rate between glycine and D-alanine can be explained in terms of radical stabilisation. The destruction mechanism of glycine, suggested by Ehrenfreund *et al.* (2001b) starts with the separation of the carboxyl group:

$$H_2NCH_2COOH \xrightarrow{h\nu} H_2NCH_2^{\cdot} + {}^{\cdot}COOH$$

Rearrangement of the proton on the $H_2NCH_2^{\cdot}$ radical would lead to methylamine (CH_3NH_2) and CO_2. The stability of this intermediate radical determines the rate of this process. Secondary and tertiary radicals appear to be more stable than primary radicals. The ethylamine radical ($H_2NC_2H_4^{\cdot}$) made from D-alanine is therefore more stable and so D-alanine breaks down more rapidly than glycine.

From these results we attempted to obtain knowledge on how long amino acids could survive when embedded into the martian regolith. Our measured reaction rates can be used to calculate estimated decomposition rates for amino acids on Mars. Using first-order decomposition kinetics the concentration of amino acids at a given time can be calculated from Equation 1:

$$N_t = N_0 \, e^{-Jt} \qquad (1)$$

where J is the destruction rate, a function of the destruction cross section and the flux. N_t is the concentration (number of

molecules) at time t, N_0 the initial concentration and t the time (s). From this relationship we can estimate the time it takes for an initial regolith load of 1 ppb of amino acids in the martian regolith to decrease to less than 1 part per trillion (ppt, 1 per 10^{12}). With an attenuation of the destruction rate by a factor of 10^9, which is equivalent to the assumed regolith dilution ratio and caused by the shielding effect of the regolith, the level of amino acids would decrease from 1 ppb to 1 ppt in approximately 4×10^7 years for glycine and 5×10^6 years for D-alanine, in the absence of regolith mixing and additional amino acid inputs. This calculation represents the expected lower limit of the possible decrease in destruction rate due to dilution of amino acids in the regolith. An important indication of this result is that the decomposition rate is not determined by complexity of the compound. The relationship between decomposition and decrease in reaction efficiency due to regolith dilution effects by erosion are shown in Fig. 9. Continuous amino acid input to the regolith from meteoritic infall and weathering processes are not considered in Fig. 9. The actual concentration of organics in the martian regolith is expected to depend on the balance between the photodecomposition rate and the input rate of amino acids due to physical weathering and mixing occurring on the planet's surface. Physical weathering (processes that break down or fragment rocks and minerals) has many causes, including particle collisions, impact cratering, glacial processes, and volcanism. Currently, it appears that Mars is far less geologically active than it has been in the past and it is likely that the primary mechanism of physical weathering on Mars today is aeolian erosion caused by the collision of particles moved by wind. Missions to Mars have returned evidence of the extent to which aeolian activity is currently occurring on Mars. Bridges *et al.* (1999) determined that approximately half of the rocks at the Mars Pathfinder site has been abraded by wind-borne particles. Although the Pathfinder site was formed by an ancient out-flow channel, aeolian resurfacing of the site has clearly occurred and is likely to be the dominant geological process occurring on the planet today. The rate of physical weathering determines the rate at which fresh surfaces are exposed to UV light. Once a surface is exposed, chemical weathering may proceed through UV induced oxidation process.

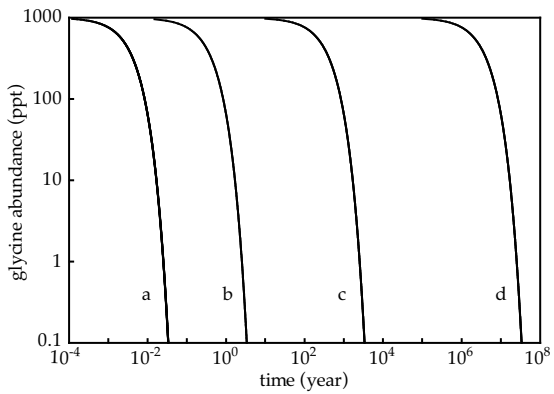

Fig 9. The concentration of glycine in the regolith as a function of time. The lines show the rates for different levels of destruction cross section attenuation due to dilution of the amino acid in the regolith. Levels of attenuation: (a) 1, (b) 10^2, (c) 10^5, (d) 10^9.

Carr (1992) has estimated the average rate of deposition due to physical erosion on Mars to be 20 nm yr^{1}, which corresponds to an approximate rate of 5×10^{-5} kg m^{-2} yr^{-1}. Assuming that surface rocks contain 1 ppb of amino acids, the erosional contribution to the regolith would be 50 picograms of amino acid m^{-2} yr^{-1}. For accumulation of amino acids in the regolith to occur, input rates must exceed photodecomposition rates. Assuming a 2 μm penetration depth of UV photons into the regolith, this condition is met when attenuation of the measured destruction cross section is greater than 10^{5}. In cases where the attenuation is below 10^{5}, amino acids are removed more rapidly than the input rate.

It is reasonable to expect the decomposition rate of amino acids in the regolith on Mars to exceed the input rate, since the effective attenuation of the destruction cross section will likely be lower than the dilution ratio due to UV scattering by the regolith. There may be a further enhancement in the degradation rate resulting from catalytic regolith surfaces (Quinn and Zent, 1999).

There are two previously published laboratory studies that examined the photostability of amino acids in the martian surface material; in both cases only glycine was studied. Oró and Holzer (1979) demonstrated the UV decomposition of pure glycine in the presence of small amounts of O_2 gas in a dry nitrogen atmosphere. In their experiments 95 % of the glycine was recovered after 10^{9} hours of illumination at Mars flux levels. No decomposition of glycine was observed in samples irradiated in dry nitrogen. Stoker and Bullock (1997) measured the photodecomposition of glycine mixed in a palagonitic regolith in the presence of a simulated martian atmosphere and attributed their results to the effects of UV alone. Stoker and Bullock (1997) concluded that the presence of oxidising agents is not needed to explain the depleted level of organics in martian Viking regolith samples. This conclusion is at odds with the results of Oró and Holzer (1979). The decomposition rates reported in this paper are consistent with the results of Oró and Holzer (1979) for glycine decomposition in the presence of low levels of oxygen, indicating that radical induced decomposition mechanisms may have also played a role in our observed rates.

In our amino acid films, a limited amount of H_2O molecules may be incorporated in the amino acid thin films during deposition and/or irradiation. The irradiation of H_2O molecules can lead to the generation of OH and other strongly oxidising radicals. The photochemical production of oxidizing radicals both in the near-surface atmosphere, and on exposed surface material, is thought to play a major role in the decomposition of organics on Mars (Zent and McKay, 1994). The background pressure in the simulation chamber during sample exposure to UV light was $< 10^{-5}$ mbar. In high vacuum systems the residual gas is predominately water and at 10^{-5} mbar the partial pressure of water corresponds to the approximately 1 part per million (ppm) of water vapour in the martian atmosphere. Therefore, the background gas phase water abundance in the chamber is consistent with Mars number densities and the uniformity of the IR spectra and the repeatability of the measured half-lives indicates that the water abundance in -

corporated into the samples is small, constant and not greater than expected Mars abundances.

This work is part of a comprehensive multi-year effort to describe the response of biologically important molecules to planetary environments, and in particular that of the martian surface. Studying the survival of endogenous or exogenous bio-relevant compounds involves multi-parameter simulations, of which the atmospheric interactions with the UV lighting found at Mars are of special interest and will be examined in future work.

5. Conclusions

We have constructed a system that allows *in situ* measurements of the destruction rates of amino acid in solid thin films exposed to UV radiation. These rates have been used to predict the decomposition rates of two amino acids, glycine and D-alanine, on the surface of Mars. We estimate that for a starting amino acid load of 1 ppb in the martian regolith, the amino acid concentration would decrease to less than 1 part per trillion (ppt) in approximately 4×10^{7} years for glycine and 5×10^{6} years for D-alanine. Additionally, for accumulation of amino acids from weathering processes to occur in the regolith, our measured destruction rate for pure glycine would have to be attenuated by a factor of 10^{5} by regolith mixing. Given this attenuation factor combined with the additional rate increase that is expected due to radical generation in the regolith by UV, decomposition of amino acids is expected to outstrip accumulation on the surface of Mars.

Attempts to detect organic compounds by the Viking landers were unsuccessful and indicated that the surface samples contained no detectable amount of native organic material. These *in situ* results along with our laboratory measurements indicate that levels of amino acids in the martian regolith are likely to be below the ppt level. Successful detection of organic compounds on Mars will require highly sensitive instrumentation such as the Mars Organic Analyzer (Skelley *et al.*, 2005). Instrumentation with high sensitivity to organics, coupled with measurements designed to understand oxidative mechanisms occurring in the regolith (Zent *et al.*, 2003), represent a promising strategy for understanding Mars carbon chemistry.

Acknowledgements

The authors wish to thank J. Romstedt for providing the AFM pictures. ILtK is supported by the BioScience Initiative of Leiden University, JG is supported by the SRON National Institute for Space Research, PE and ZP are supported by grant NWO-VI 016.023.003, RQ is supported by NASA Ames cooperative agreement NCC2-1408.